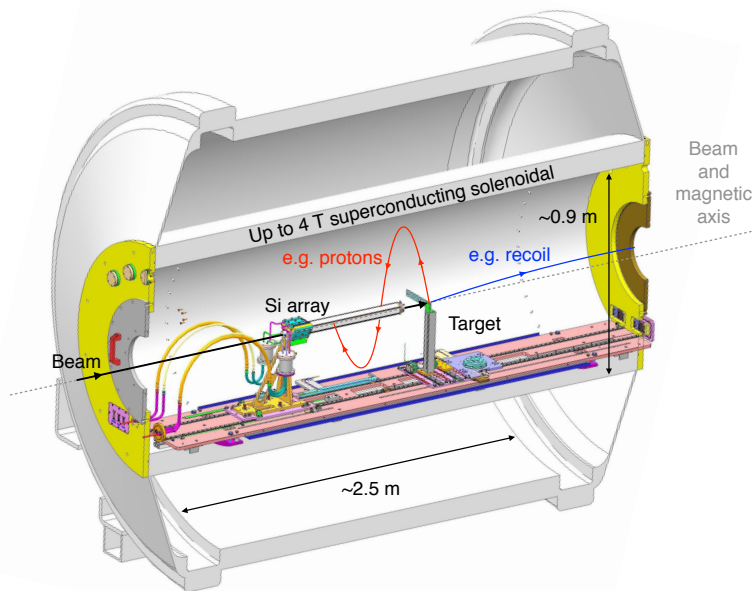


The $^{61}\text{Zn}(d,p)^{62}\text{Zn}$ transfer reaction and other nuclear astrophysics opportunities with the ISS

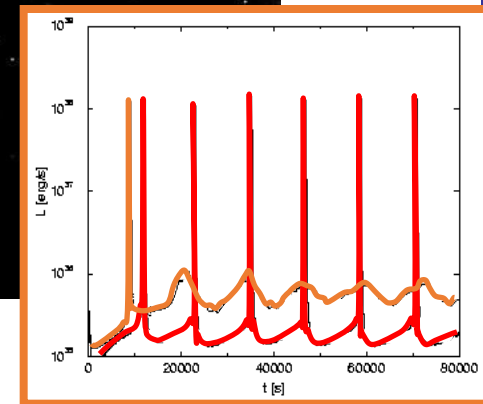
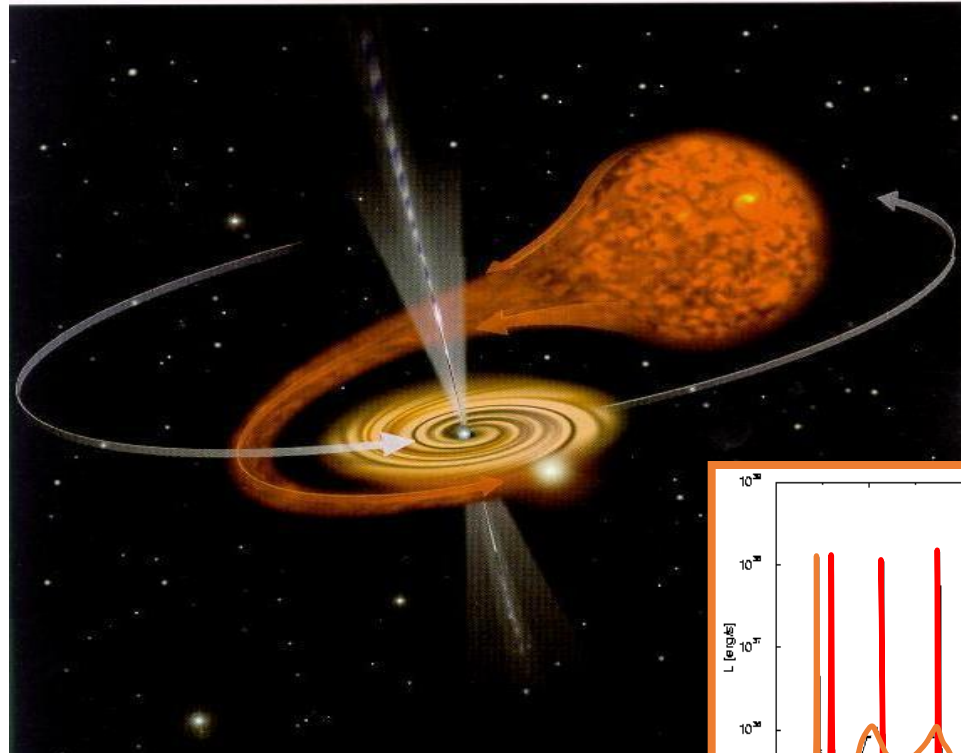
Daniel Doherty
University of Surrey
ISS Meeting, August 2019



Motivation

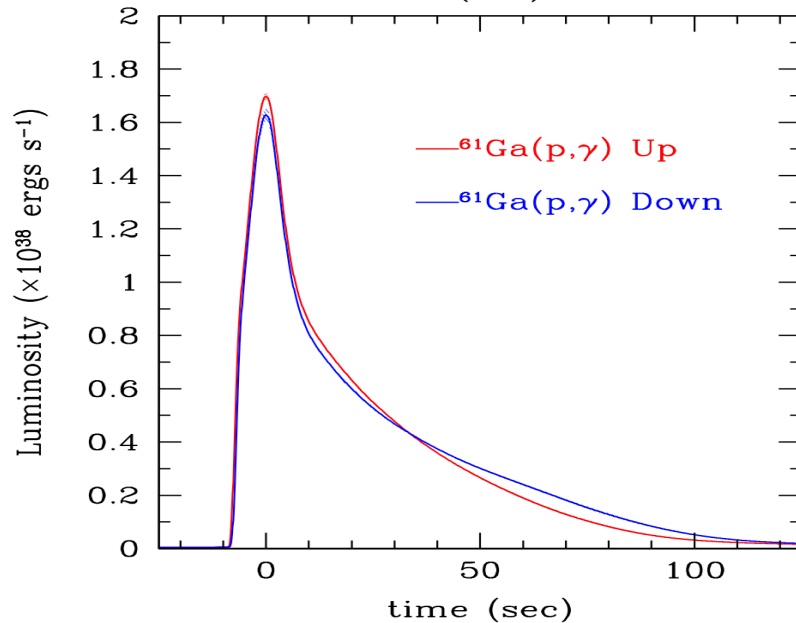
The observation of X-ray bursts is interpreted as thermonuclear explosions in the atmosphere of a neutron star in a close binary system.

As temperature and density at the surface of the neutron star increase, the CNO cycles breakout into the *rp* process.

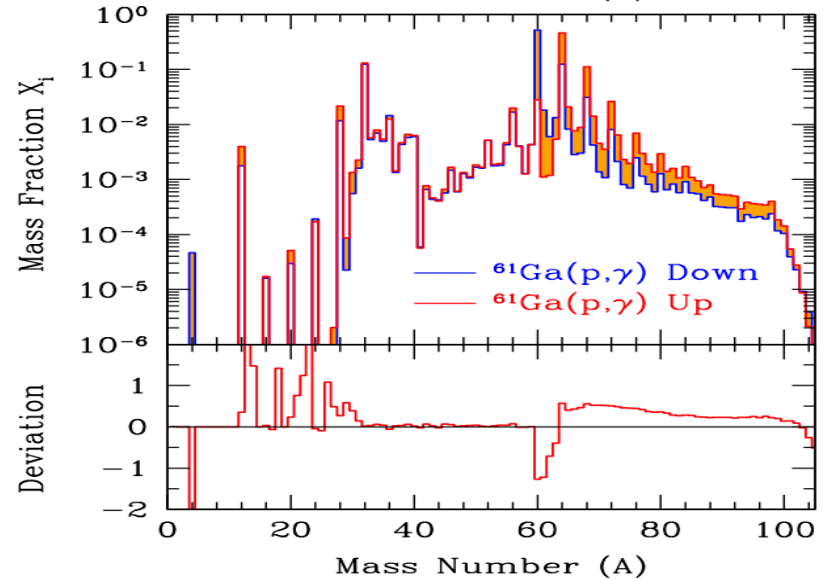


Sensitivity studies highlight the key reactions for understanding these bursts
 $\rightarrow {}^{61}\text{Ga}(p, \gamma){}^{62}\text{Ge}$ suggested as being particularly important

Motivation



Effect on the X-ray burst light curve from varying the $^{61}\text{Ga}(p,\gamma)^{62}\text{Ge}$ reaction rate within its associated uncertainties.



Effect on the final abundances from varying the $^{61}\text{Ga}(p,\gamma)^{62}\text{Ge}$ reaction rate within its associated uncertainties.

Motivation

TABLE 19

SUMMARY OF THE MOST INFLUENTIAL NUCLEAR PROCESSES, AS COLLECTED FROM TABLES 1–10

Reaction	Models Affected
$^{12}\text{C}(\alpha, \gamma)^{16}\text{O}^{\text{a}}$	F08, K04-B2, K04-B4, K04-B5
$^{18}\text{Ne}(\alpha, p)^{21}\text{Na}^{\text{a}}$	K04-B1 ^b
$^{25}\text{Si}(\alpha, p)^{28}\text{P}$	K04-B5
$^{26}\text{gAl}(\alpha, p)^{29}\text{Si}$	F08
$^{29}\text{S}(\alpha, p)^{32}\text{Cl}$	K04-B5
$^{30}\text{P}(\alpha, p)^{33}\text{S}$	K04-B4
$^{30}\text{S}(\alpha, p)^{33}\text{Cl}$	K04-B4, ^b K04-B5 ^b
$^{31}\text{Cl}(p, \gamma)^{32}\text{Ar}$	K04-B1
$^{32}\text{S}(\alpha, \gamma)^{36}\text{Ar}$	K04-B2
$^{56}\text{Ni}(\alpha, p)^{59}\text{Cu}$	S01, ^b K04-B5
$^{57}\text{Cu}(p, \gamma)^{58}\text{Zn}$	F08
$^{59}\text{Cu}(p, \gamma)^{60}\text{Zn}$	S01, ^b K04-B5
$^{61}\text{Ga}(p, \gamma)^{62}\text{Ge}$	F08, K04-B1, K04-B2, K04-B5, K04-B6
$^{65}\text{As}(p, \gamma)^{66}\text{Se}$	K04, ^b K04-B1, K04-B2, ^b K04-B3, ^b K04-B4, K04-B5, K04-B6
$^{69}\text{Br}(p, \gamma)^{70}\text{Kr}$	K04-B7
$^{75}\text{Rb}(p, \gamma)^{76}\text{Sr}$	K04-B2
$^{82}\text{Zr}(p, \gamma)^{83}\text{Nb}$	K04-B6
$^{84}\text{Zr}(p, \gamma)^{85}\text{Nb}$	K04-B2
$^{84}\text{Nb}(p, \gamma)^{85}\text{Mo}$	K04-B6
$^{85}\text{Mo}(p, \gamma)^{86}\text{Tc}$	F08
$^{86}\text{Mo}(p, \gamma)^{87}\text{Tc}$	F08, K04-B6
$^{87}\text{Mo}(p, \gamma)^{88}\text{Tc}$	K04-B6
$^{92}\text{Ru}(p, \gamma)^{93}\text{Rh}$	K04-B2, K04-B6
$^{93}\text{Rh}(p, \gamma)^{94}\text{Pd}$	K04-B2
$^{96}\text{Ag}(p, \gamma)^{97}\text{Cd}$	K04, K04-B2, K04-B3, K04-B7
$^{102}\text{In}(p, \gamma)^{103}\text{Sn}$	K04, K04-B3
$^{103}\text{In}(p, \gamma)^{104}\text{Sn}$	K04-B3, K04-B7
$^{103}\text{Sn}(\alpha, p)^{106}\text{Sb}$	S01 ^b

Motivation

TABLE 19

SUMMARY OF THE MOST INFLUENTIAL NUCLEAR PROCESSES, AS COLLECTED FROM TABLES 1–10

Reaction	Models Affected
$^{12}\text{C}(\alpha, \gamma)^{16}\text{O}^{\text{a}}$	F08, K04-B2, K04-B4, K04-B5
$^{18}\text{Ne}(\alpha, p)^{21}\text{Na}^{\text{a}}$	K04-B1 ^b
$^{25}\text{Si}(\alpha, p)^{28}\text{P}$	K04-B5
$^{26g}\text{Al}(\alpha, p)^{29}\text{Si}$	F08
$^{29}\text{S}(\alpha, p)^{32}\text{Cl}$	K04-B5
$^{30}\text{P}(\alpha, p)^{33}\text{S}$	K04-B4
$^{30}\text{S}(\alpha, p)^{33}\text{Cl}$	K04-B4, ^b K04-B5 ^b
$^{31}\text{Cl}(p, \gamma)^{32}\text{Ar}$	K04-B1
$^{32}\text{S}(\alpha, \gamma)^{36}\text{Ar}$	K04-B2
$^{56}\text{Ni}(\alpha, p)^{59}\text{Cu}$	S01, ^b K04-B5
$^{57}\text{Cu}(p, \gamma)^{58}\text{Zn}$	F08
$^{59}\text{Cu}(p, \gamma)^{60}\text{Zn}$	S01, ^b K04-B5
$^{61}\text{Ga}(p, \gamma)^{62}\text{Ge}$	F08, K04-B1, K04-B2, K04-B5, K04-B6
$^{65}\text{As}(p, \gamma)^{66}\text{Se}$	K04, ^b K04-B1, K04-B2, ^b K04-B3, ^o K04-B4, K04-B5, K04-B6
$^{69}\text{Br}(p, \gamma)^{70}\text{Kr}$	K04-B7
$^{75}\text{Rb}(p, \gamma)^{76}\text{Sr}$	K04-B2
$^{82}\text{Zr}(p, \gamma)^{83}\text{Nb}$	K04-B6
$^{84}\text{Zr}(p, \gamma)^{85}\text{Nb}$	K04-B2
$^{84}\text{Nb}(p, \gamma)^{85}\text{Mo}$	K04-B6
$^{85}\text{Mo}(p, \gamma)^{86}\text{Tc}$	F08
$^{86}\text{Mo}(p, \gamma)^{87}\text{Tc}$	F08, K04-B6
$^{87}\text{Mo}(p, \gamma)^{88}\text{Tc}$	K04-B6
$^{92}\text{Ru}(p, \gamma)^{93}\text{Rh}$	K04-B2, K04-B6
$^{93}\text{Rh}(p, \gamma)^{94}\text{Pd}$	K04-B2
$^{96}\text{Ag}(p, \gamma)^{97}\text{Cd}$	K04, K04-B2, K04-B3, K04-B7
$^{102}\text{In}(p, \gamma)^{103}\text{Sn}$	K04, K04-B3
$^{103}\text{In}(p, \gamma)^{104}\text{Sn}$	K04-B3, K04-B7
$^{103}\text{Sn}(\alpha, p)^{106}\text{Sb}$	S01 ^b

States of Interest in ^{62}Zn

Proton separation energy in ^{62}Ge is 2053(145) keV - uncertainty from mass data	3043 keV	_____	0^+
	2884 keV	_____	2^+
	2803 keV	_____	2^+
	2744 keV	_____	4^+
Mirror energy differences from theory	2384 keV	_____	3^+
	2330 keV	_____	0^+
Rate expected to be dominated by low-spin states	2186 keV	_____	4^+

^{62}Zn

States of Interest in ^{62}Zn

The Spectroscopic factor (C^2S) is directly related to the proton widths and, hence, the resonance strengths.

$$\omega\gamma = \omega \frac{\Gamma_p \Gamma_\gamma}{\Gamma_p + \Gamma_\gamma} \approx \omega \frac{\Gamma_p \Gamma_\gamma}{\Gamma_\gamma} \approx \omega \Gamma_p. \quad \Gamma_p = C^2 S \Gamma_{sp}$$

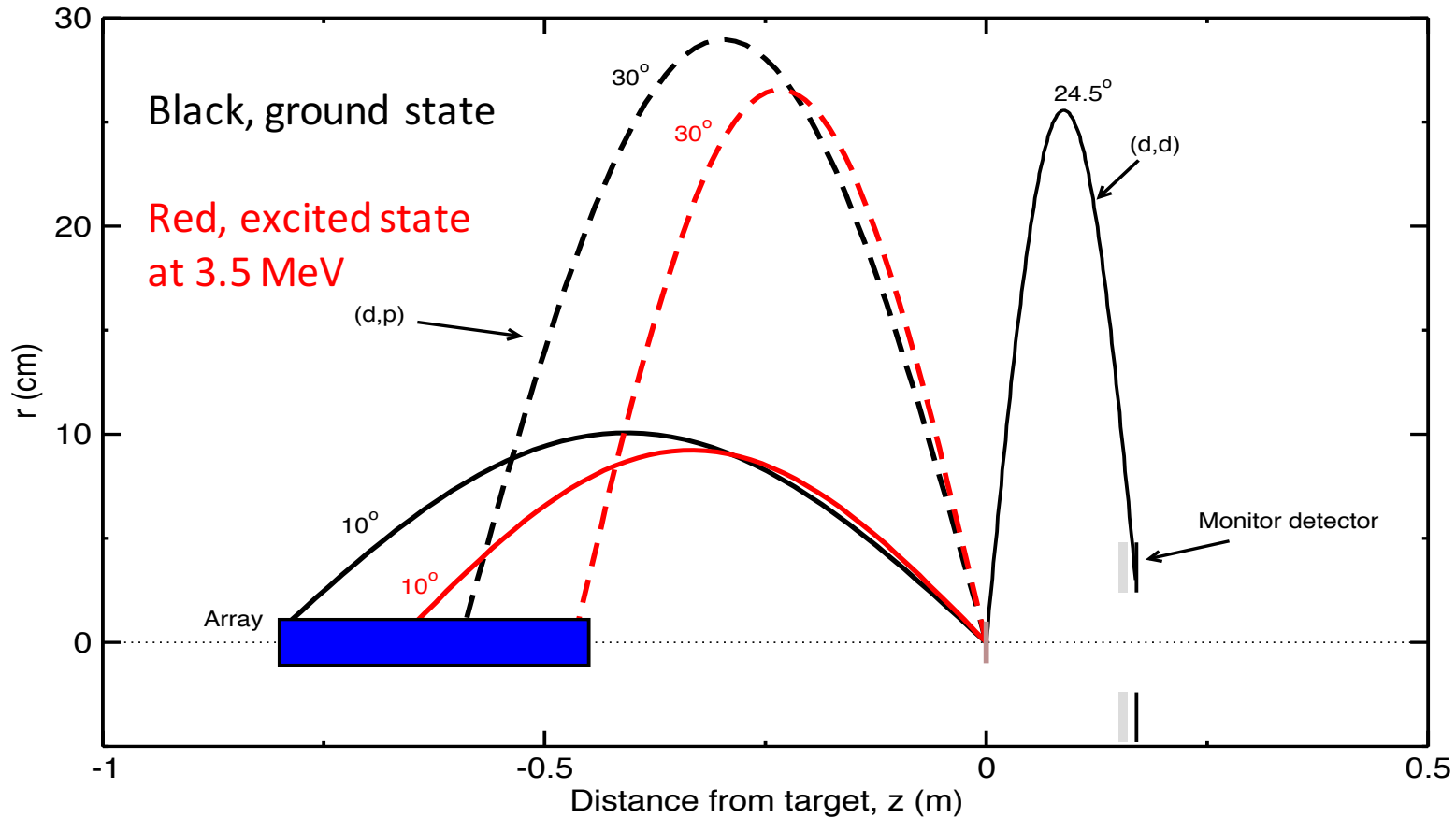
Will be extracted from the proton yields with the ADWA code TWOFNR. Recent success for the astrophysically important ^{27}Al - ^{27}Si system. V. Margerin et al., PRL **115** 062701 (2015)

C^2S of mirror analog states are expected to agree within 20%

N. K. Timofeyuk, R. C. Johnson, and A. M. Mukhamedzhanov, PRL **91**, 232501 (2003)
N. K. Timofeyuk, P. Descouvemont, and R. C. Johnson, Eur. Phys. J. A **27**, 269 (2006).

ISS – ISOLDE Solenoid Spectrometer

$d(^{61}\text{Zn},p)^{62}\text{Zn}$, 7.5 MeV/u, 2.5 T

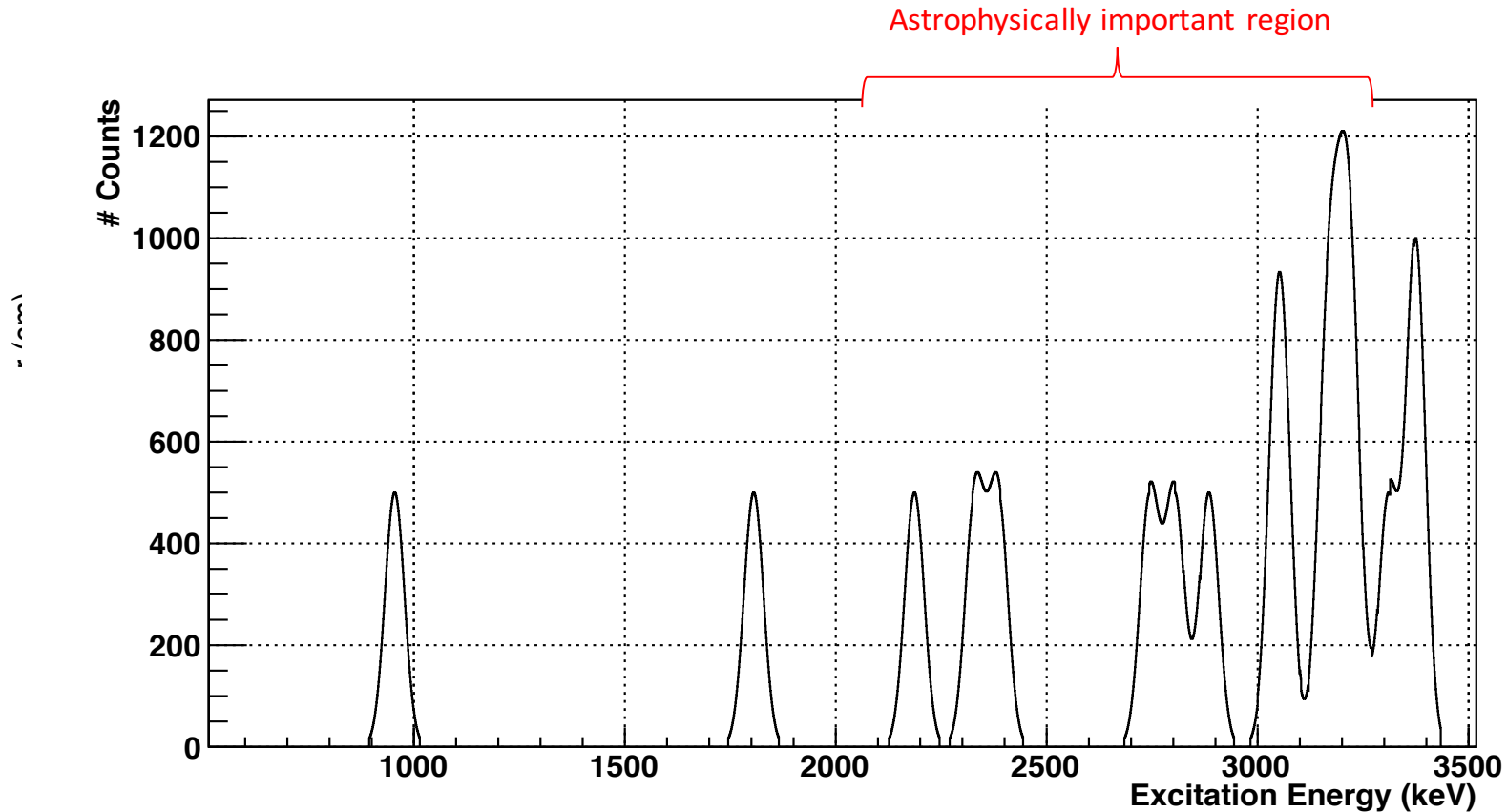


$10^\circ < \theta_{\text{CM}} < 30^\circ \Rightarrow$ protons emitted at backward lab angles

Proton energies ~ 10 MeV

ISS – ISOLDE Solenoid Spectrometer

Know ^{62}Zn level scheme folded with 75-keV resolution obtained with HELIOS type device and detectors



$10^\circ < \theta_{\text{CM}} < 30^\circ \Rightarrow$ protons emitted at backward lab angles

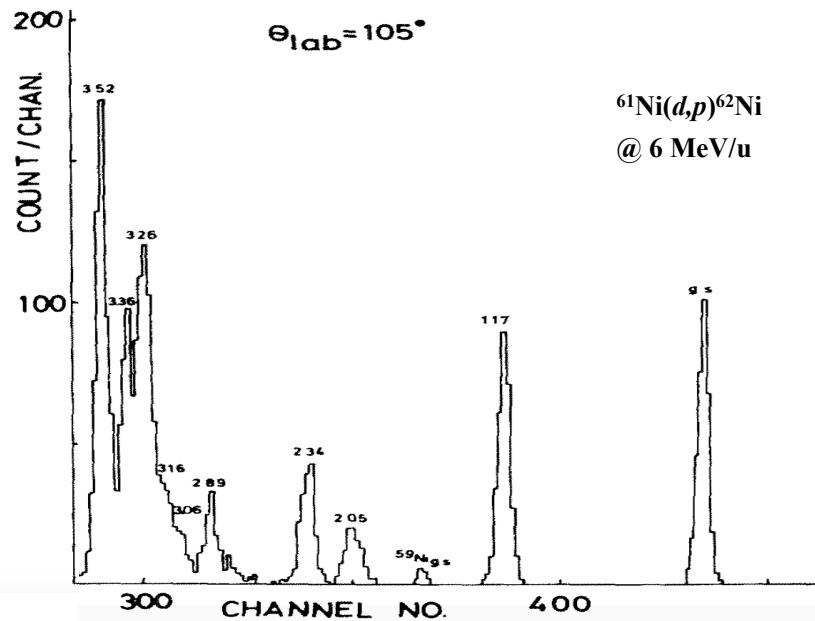
Proton energies ~ 10 MeV

ISS – ISOLDE Solenoid Spectrometer

7.5 MeV/u ^{61}Zn beam of minimum intensity 4×10^5 pps (ZrO₂ target)

Ga contamination to be suppressed with RILIS ionisation of Zn

Stable ^{61}Ni contaminant highlighted in TAC meeting, known spectrum. See below.



Problems from transfer on light elements from EBIS charge breeder?

Energy Generation in X-ray Bursts (again)

THE ASTROPHYSICAL JOURNAL, 872:84 (18pp), 2019 February 10

Influence of Nuclear Reaction Rate Uncertainties on Neutron Star Properties Extracted from X-Ray Burst Model–Observation Comparisons

Zach Meisel, Grant Merz, and Sophia Medvid

THE ASTROPHYSICAL JOURNAL, 830:55 (20pp), 2016 October 20

DEPENDENCE OF X-RAY BURST MODELS ON NUCLEAR REACTION RATES

R. H. CYBURT^{1,2}, A. M. AMTHOR³, A. HEGER^{2,4,5,6}, E. JOHNSON⁷, L. KEEK^{1,2,7,9}, Z. MEISEL^{2,8}, H. SCHATZ^{1,2,7}, AND K. SMITH^{2,10}

Reactions that Impact the Burst Light Curve
in the Multi-zone X-ray Burst Model

Rank	Reaction	Type ^a	Sensitivity ^b	Category
1	$^{15}\text{O}(\alpha, \gamma)^{19}\text{Ne}$	D	16	1
2	$^{56}\text{Ni}(\alpha, p)^{59}\text{Cu}$	U	6.4	1
3	$^{59}\text{Cu}(p, \gamma)^{60}\text{Zn}$	D	5.1	1
4	$^{61}\text{Ga}(p, \gamma)^{62}\text{Ge}$	D	3.7	1
5	$^{22}\text{Mg}(\alpha, p)^{25}\text{Al}$	D	2.3	1
6	$^{14}\text{O}(\alpha, p)^{17}\text{F}$	D	5.8	1
7	$^{23}\text{Al}(p, \gamma)^{24}\text{Si}$	D	4.6	1
8	$^{18}\text{Ne}(\alpha, p)^{21}\text{Na}$	U	1.8	1
9	$^{63}\text{Ga}(p, \gamma)^{64}\text{Ge}$	D	1.4	2
10	$^{19}\text{F}(p, \alpha)^{16}\text{O}$	U	1.3	2
11	$^{12}\text{C}(\alpha, \gamma)^{16}\text{O}$	U	2.1	2
12	$^{26}\text{Si}(\alpha, p)^{29}\text{P}$	U	1.8	2
13	$^{17}\text{F}(\alpha, p)^{20}\text{Ne}$	U	3.5	2
14	$^{24}\text{Mg}(\alpha, \gamma)^{28}\text{Si}$	U	1.2	2
15	$^{57}\text{Cu}(p, \gamma)^{58}\text{Zn}$	D	1.3	2
16	$^{60}\text{Zn}(\alpha, p)^{63}\text{Ga}$	U	1.1	2
17	$^{17}\text{F}(p, \gamma)^{18}\text{Ne}$	U	1.7	2
18	$^{40}\text{Sc}(p, \gamma)^{41}\text{Ti}$	D	1.1	2
19	$^{48}\text{Cr}(p, \gamma)^{49}\text{Mn}$	D	1.2	2

A variety of (p, γ) and (α, p) reactions have significant affect on the energy generated in X-ray bursts.

KEY REACTIONS

1. $^{61}\text{Ga}(p, \gamma)^{62}\text{Ge}$
2. $^{22}\text{Mg}(\alpha, p)^{25}\text{Al}$
3. $^{14}\text{O}(\alpha, p)^{17}\text{F}$
4. $^{17}\text{F}(\alpha, p)^{20}\text{Ne}$
5. $^{18}\text{Ne}(\alpha, p)^{21}\text{Na}$
6. $^{60}\text{Zn}(\alpha, p)^{63}\text{Ga}$
7. $^{57}\text{Cu}(p, \gamma)^{58}\text{Zn}$

Energy Generation in X-ray Bursts (again)

THE ASTROPHYSICAL JOURNAL, 872:84 (18pp), 2019 February 10

Influence of Nuclear Reaction Rate Uncertainties on Neutron Star Properties Extracted from X-Ray Burst Model–Observation Comparisons

Zach Meisel, Grant Merz, and Sophia Medvid

However, (α, p) reactions require a new development...

in the Multi-zone X-ray Burst Model

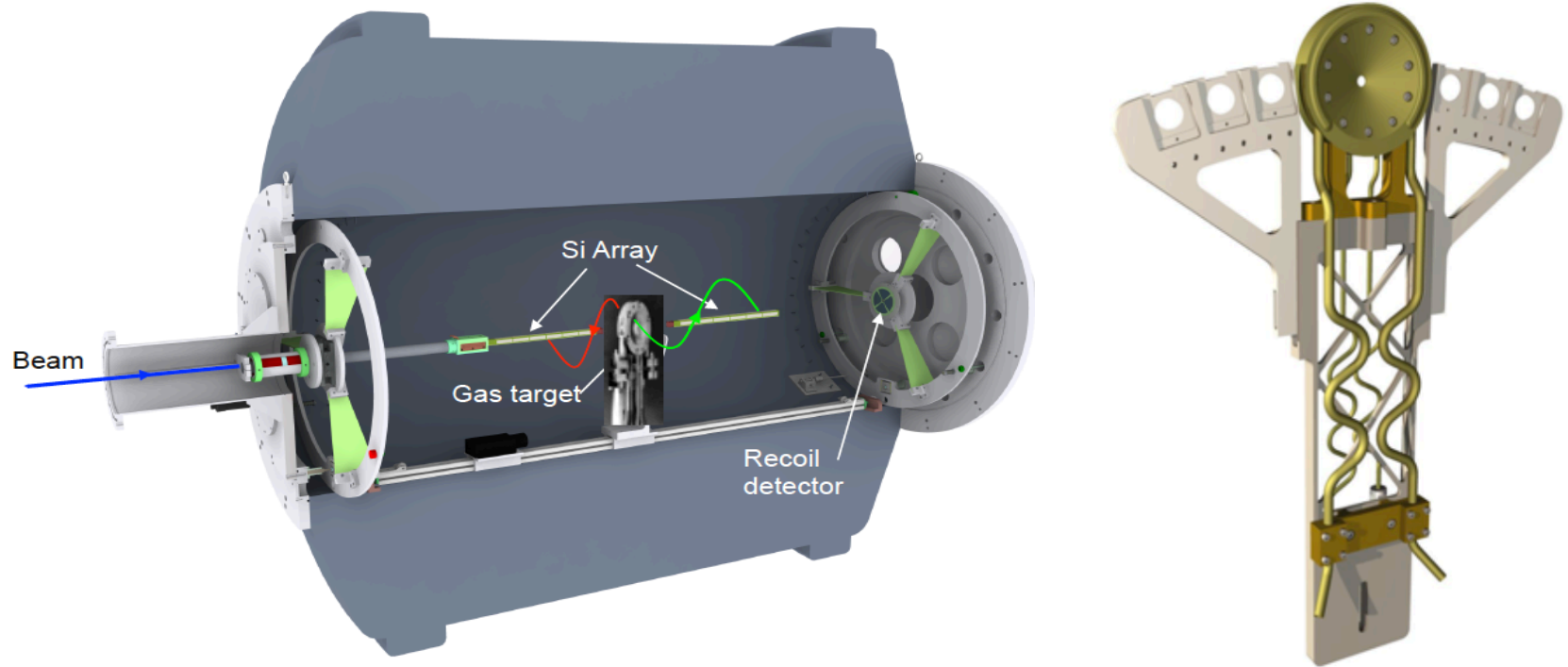
Rank	Reaction	Type ^a	Sensitivity ^b	Category
1	$^{15}\text{O}(\alpha, \gamma)^{19}\text{Ne}$	D	16	1
2	$^{56}\text{Ni}(\alpha, p)^{59}\text{Cu}$	U	6.4	1
3	$^{59}\text{Cu}(p, \gamma)^{60}\text{Zn}$	D	5.1	1
4	$^{61}\text{Ga}(p, \gamma)^{62}\text{Ge}$	D	3.7	1
5	$^{22}\text{Mg}(\alpha, p)^{25}\text{Al}$	D	2.3	1
6	$^{14}\text{O}(\alpha, p)^{17}\text{F}$	D	5.8	1
7	$^{23}\text{Al}(p, \gamma)^{24}\text{Si}$	D	4.6	1
8	$^{18}\text{Ne}(\alpha, p)^{21}\text{Na}$	U	1.8	1
9	$^{63}\text{Ga}(p, \gamma)^{64}\text{Ge}$	D	1.4	2
10	$^{19}\text{F}(p, \alpha)^{16}\text{O}$	U	1.3	2
11	$^{12}\text{C}(\alpha, \gamma)^{16}\text{O}$	U	2.1	2
12	$^{26}\text{Si}(\alpha, p)^{29}\text{P}$	U	1.8	2
13	$^{17}\text{F}(\alpha, p)^{20}\text{Ne}$	U	3.5	2
14	$^{24}\text{Mg}(\alpha, \gamma)^{28}\text{Si}$	U	1.2	2
15	$^{57}\text{Cu}(p, \gamma)^{58}\text{Zn}$	D	1.3	2
16	$^{60}\text{Zn}(\alpha, p)^{63}\text{Ga}$	U	1.1	2
17	$^{17}\text{F}(p, \gamma)^{18}\text{Ne}$	U	1.7	2
18	$^{40}\text{Sc}(p, \gamma)^{41}\text{Ti}$	D	1.1	2
19	$^{48}\text{Cr}(p, \gamma)^{49}\text{Mn}$	D	1.2	2

A variety of (p, γ) and (α, p) reactions have significant affect on the energy generated in X-ray bursts.

KEY REACTIONS

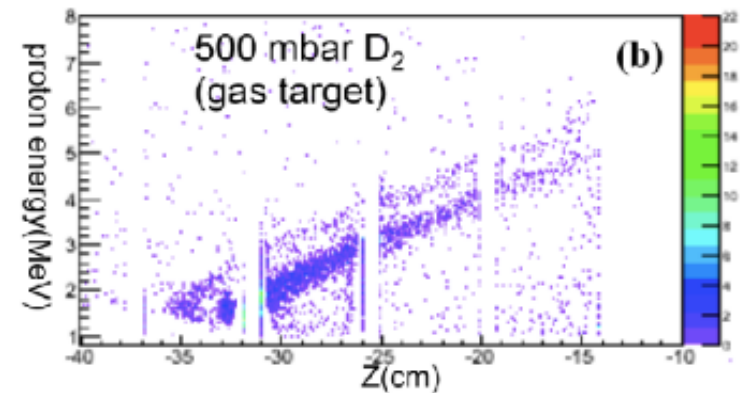
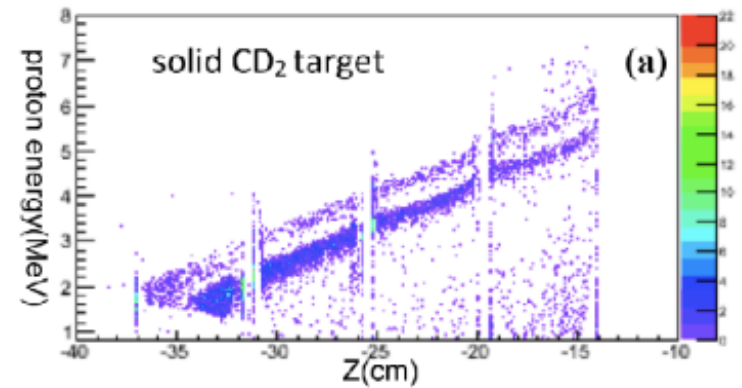
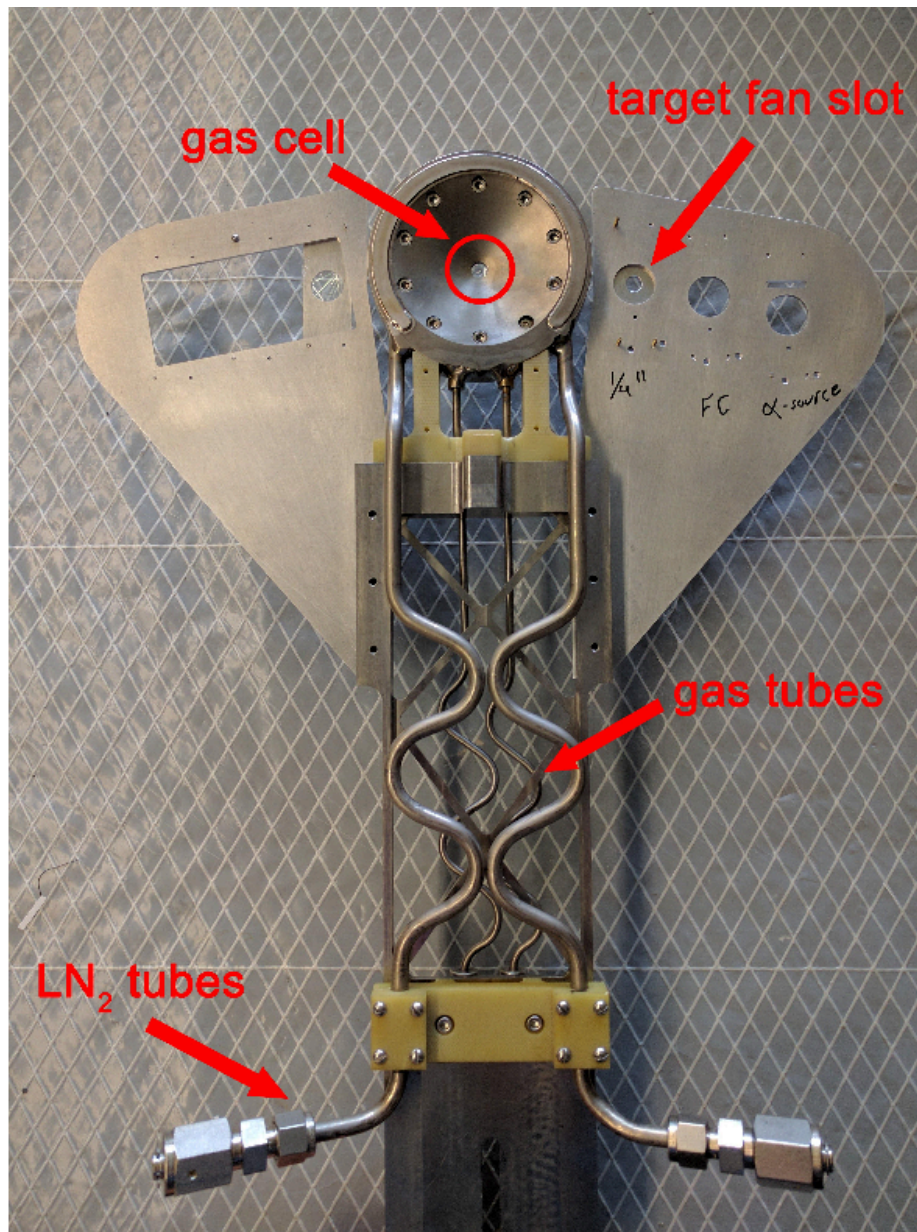
1. $^{61}\text{Ga}(p, \gamma)^{62}\text{Ge}$
2. $^{22}\text{Mg}(\alpha, p)^{25}\text{Al}$
3. $^{14}\text{O}(\alpha, p)^{17}\text{F}$
4. $^{17}\text{F}(\alpha, p)^{20}\text{Ne}$
5. $^{18}\text{Ne}(\alpha, p)^{21}\text{Na}$
6. $^{60}\text{Zn}(\alpha, p)^{63}\text{Ga}$
7. $^{57}\text{Cu}(p, \gamma)^{58}\text{Zn}$

Development of Cryogenic Target for ISS



- Could improve upon HELIOS design shown above, although the option to change gas targets quickly is certainly useful.
- Currently uses Kapton windows
- Target thickness $\sim 50 \mu\text{g}/\text{cm}^2$
- Ability to accurately identify recoils is crucial (e.g. Ion Chamber)

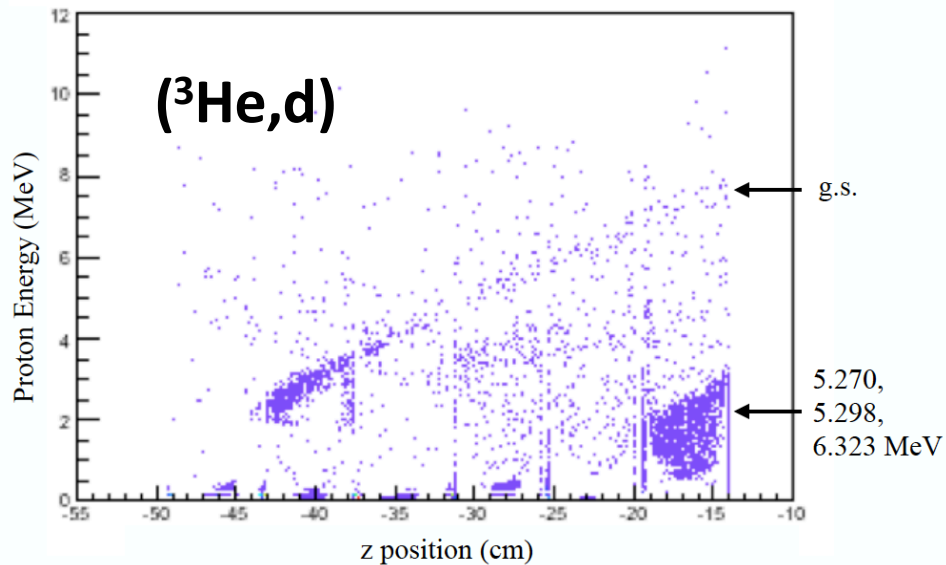
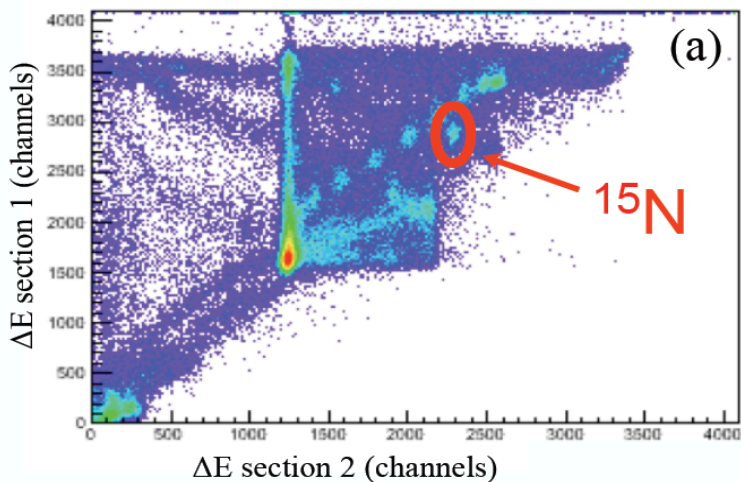
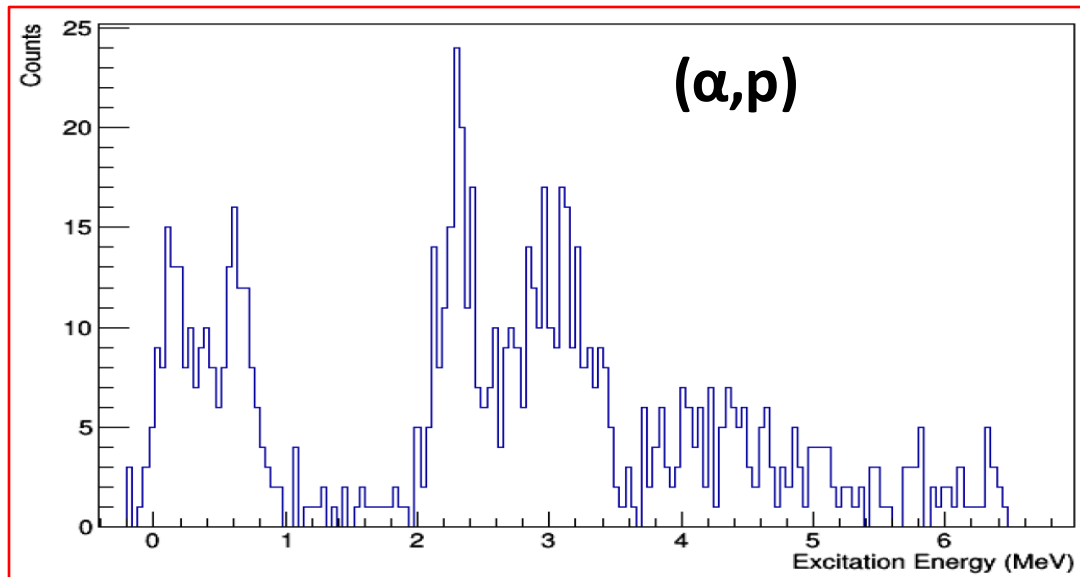
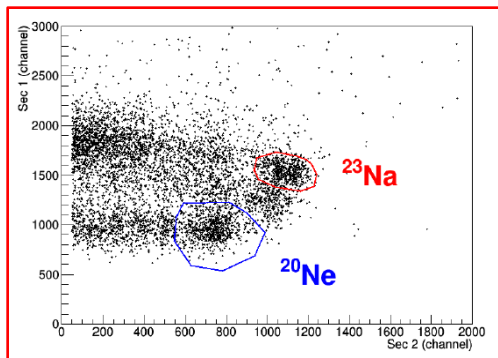
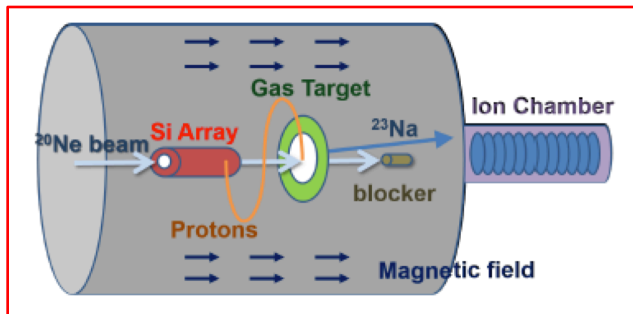
HELIOS Cryogenic Target



Proton spectra from $d(^{14}\text{C},p)^{15}\text{C}$ reaction

J. Lai, PhD Thesis, LSU (2016)

Previous Studies of $^{20}\text{Ne}(\alpha,p)$ and $^{14}\text{C}(^3\text{He},d)$

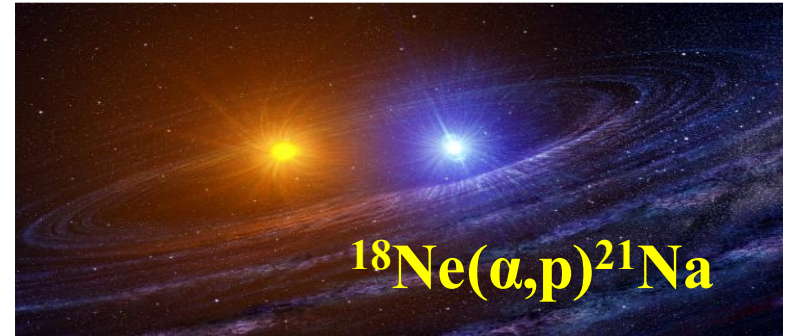
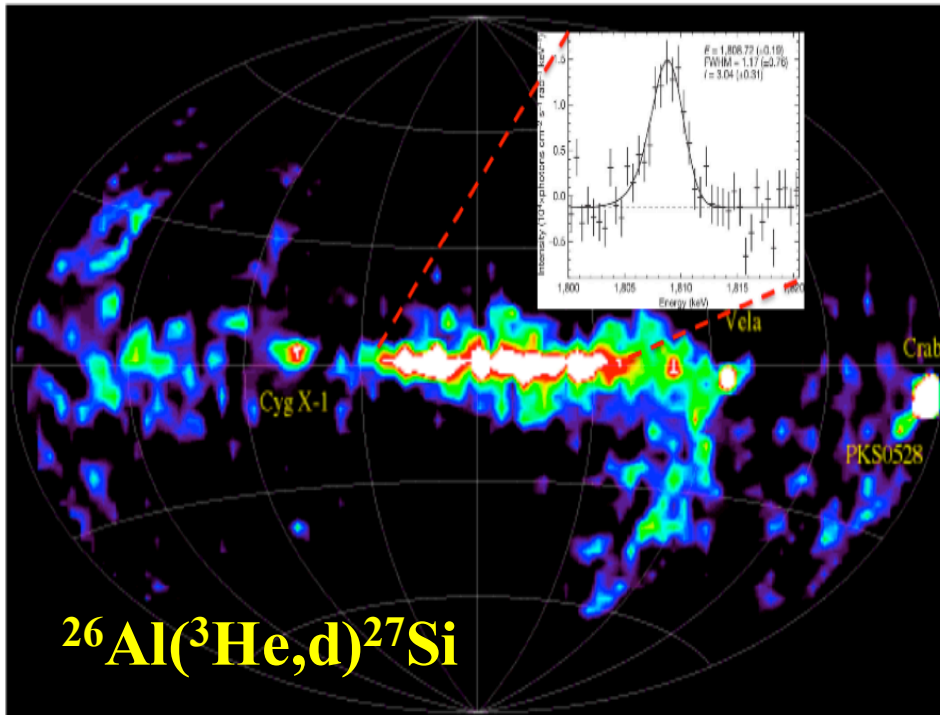


Challenges and Discussion Points

- Gas targets are extremely challenging but the rewards are substantial and makes good use of the unique beam species available at HIE-ISOLDE.
- Work underway to look at new types of target, different windows etc (mentioned by Calem yesterday)
- Beam energies relatively low ($< 2 \text{ Mev/u}$)
- Need normalization for (α, p) measurements
 $\Rightarrow (\alpha, \alpha')$

Summary

- A number of opportunities already exist for performing astrophysically important measurements using the ISS [e.g. $^{61}\text{Zn}(d,p)^{62}\text{Zn}$]
- However, the development of a cryogenic target would open up a whole host of possibilities in terms of nuclear astrophysics [e.g. some of the first direct measurements of (α,p) process reactions]



Thank you very much!

G. Lotay¹, **D.T. Doherty**¹, W.N. Catford¹, Zs. Podolyak¹, P.A. Butler², R.D. Page², D.K. Sharp³, S.J. Freeman³, M. Labiche⁴, B.P. Kay⁵, C.R. Hoffman⁵, R.V.F. Janssens⁵, D.G. Jenkins⁶, N. Orr⁷, A. Matta⁷,
⁸L. P. Gaffney

¹*Department of Physics, University of Surrey, Guildford, Surrey, GU2 7XH. UK.*

²*Oliver Lodge Laboratory, University of Liverpool, Liverpool, L69 7ZE, UK.*

³*School of Physics and Astronomy, University of Manchester, Manchester, M13 9PL. UK.*

⁴*STFC Daresbury Laboratory, Daresbury, Warrington, WA4 4AD. UK.*

⁵*Physics Division, Argonne National Laboratory, Argonne, Illinois, 60439. USA.*

⁶*Department of Physics, University of York, Heslington, York, YO10 5DD. UK.*

⁷*LPC-ENSICAEN, IN2P3/CNRS et Universite de Caen, 1405 Caen, FRANCE.*

⁸ *ISOLDE, CERN*

ISS – ISOLDE Solenoid Spectrometer

- 4T superconducting solenoid.
- Obtained as MRI magnet from Brisbane.
 - Arrived @ CERN in April 2016.
- Dedicated to transfer reactions with HIE-ISOLDE.
- New Si array designed and under construction (ready after LS2).
 - First experiments with ANL array.

